Modes and Their Stability of a Symmetric Two-Element Coupled Negative Conductance Oscillator Driven Spatial Power Combining Array

Zhengping Ding, *Student Member, IEEE,* and Kai Chang, *Fellow, IEEE*

Abstract—**The modes and their stability of a symmetric two-element coupled negative conductance oscillator driven spatial power combining array were addressed theoretically. It was shown that the symmetric two-element spatial power combining array can produce two stable operation modes, one in-phase, the other 180°-out-of-phase. The theory explains all previously published experimental phenomena. Experiments done at C-band with a symmetric two-element coupled Gunn oscillator driven spatial power combining array demonstrated the validity of the theory to a certain extent. The theory can be generalized to study the modes and their stability of any coupled oscillator driven spatial power combining arrays.**

I. Introduction

IN MICROWAVE and millimeter wave bands, available output powers from single solid state devices, such as Gunn diodes, are getting smaller and smaller as the frequency increases. Therefore, microwave/millimeter wave solid state source power combining becomes important [1]. In this area, quasi-optical cavity power combining proposed by Mink in 1986 [2] and spatial power combining proposed by Staiman *et al.* in 1968 [3] appear attractive because of their inherent low loss features. Without the quasi-optical cavity, spatial power combining array is more compact and efficient and has broader bandwidth than quasi-optical cavity power combining system.

Spatial power combining is such a concept that by exciting the elements of an antenna array with signals of certain phase relationship directly from solid state RF power oscillators or amplifiers, a desired beam which contains most of the radiated power will be formed. Without extra cavities, transmission lines, and phase shifters, all of which cause losses, this method can achieve high combining efficiency.

The earliest spatial power combining array was of amplifier type proposed by Staiman. Later on in 1981, Durkin *et al.* [4] synthesized a 35 GHz spatial power combining aperture array using pulsed IMPATT diode oscillators which were injection locked to a two-stage exciter to produce a broadside radiation beam. This design can still be seen as amplifier driven spatial power combining array insofar as the pulsed IMPATT diode oscillators acted as injection locked amplifiers.

In 1986, Dinger *et al.* [5] started utilizing parasitic coupling between elements of an array to injection lock all oscillators driving the elements to form a broadside radiation beam. With only the center element driven by an external signal, their design was closer to coupled oscillator-only driven spatial power combining array than Durkin *et al.*'s work. Before long, Stephan [6] also suggested using interoscillator coupling to achieve spatial power combining array. With a two-element coupled negative conductance oscillator driven spatial power combining array, Young and Stephan found that the moding problem in traditional cavity power combining technology also occurred in this kind of spatial power combining arrays [7] and [8]. Hummer and Chang carried out some experimental work with Gunn diodes mounted directly in microstrip patch antennas to form a two-element coupled Gunn oscillator driven spatial power combining array [9] and [10]. They also noticed two modes (one is in-phase, the other 180°-out-of-phase) by measuring the radiation patterns of the array.

Since then, more research work have been done in this regard [11]–[17]. But most of the analysis were based on different overly simplified theoretical models, thus, failed to yield a complete, consistent, and persuasive explanation to the modes and their stability of the seemingly promising coupled negative conductance oscillator driven spatial power combining arrays.

Therefore, in spite of those previous different analytical work, it is still necessary to seek a unified treatment of the modes and their stability of the coupled negative conductance oscillator driven spatial power combining arrays. As an attempt to this end, the modes and their stability of a symmetric two-element coupled negative conductance oscillator driven spatial power combining array are considered theoretically in this paper. At first, the very general circuit equations of the symmetric two-element spatial power combining array will be given in terms of the mutual admittance matrix of the array. It will be shown that the two modes (one in-phase, the other 180°-out-of-phase) of the symmetric two-element spatial power combining array are just two natural solutions of the circuit equations. Then, by extending Kurokawa's theory on the stability of oscillators [18] and [19], the stability of the two modes of the symmetric two-element spatial power combining array will be discussed thoroughly. The theory can explain all previously published experimental phenomena. Experiments done at C band with a symmetric two-element coupled Gunn oscillator driven spatial power combining array demonstrated the validity of the theoretical analysis to a certain extent. It is expected that the theory on the modes and their stability of

Manuscript received June 10, 1995; revised June 14, 1996. This work was supported in part by the Army Research Office.
The authors are with the Department of Electrical Engineering Texas A&M University College Station, TX 77843-3128 USA.
Publisher Item Identifier S 0018-9480(96)06897-4.

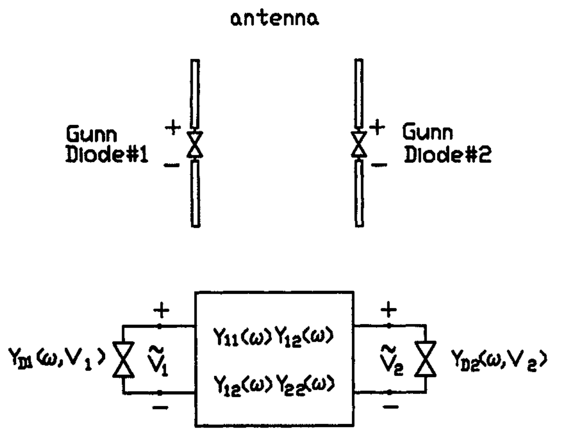

Fig. 1. A two-element coupled negative conductance oscillator driven spatial power combining array.

any (symmetric or asymmetric) coupled negative conductance oscillator driven spatial power combining array with more than two elements can be developed from similar procedures as outlined in this paper.

II. Modes and Their Stability

For a general two-element coupled negative conductance oscillator driven spatial power combining array as shown in Fig. 1, its circuit equations can be written as follows:

$$-Y_{D1}(\omega, V_1)\tilde{V}_1 = Y_{11}(\omega)\tilde{V}_1 + Y_{12}(\omega)\tilde{V}_2 \quad (1a)$$

$$-Y_{D2}(\omega, V_2)\tilde{V}_2 = Y_{21}(\omega)\tilde{V}_1 + Y_{22}(\omega)\tilde{V}_2 \quad (1b)$$

where $Y_{D1}(\omega, V_1)$ and $Y_{D2}(\omega, V_2)$ represent the admittances of the two negative conductance devices in the array, $Y_{11}(\omega)$, $Y_{12}(\omega)$, $Y_{21}(\omega)[=Y_{12}(\omega)]$, and $Y_{22}(\omega)$ are the network parameters of the passive portion of the array, ω is the angular operation frequency of the array, $\tilde{V}_1$and $\tilde{V}_2$ are the voltage phasors of the array, i.e.,

$$\tilde{V}_1 = V_1 e^{j\phi_1} \quad (2a)$$

$$\tilde{V}_2 = V_2 e^{j\phi_2} \quad (2b)$$

where V_1, V_2, ϕ_1, and ϕ_2 are the magnitudes and phases of the two voltage phasors.

From (1a), (1b), (2a), and (2b), we further have

$$-Y_{D1}(\omega, V_1) = Y_{11}(\omega) + Y_{12}(\omega)\left(\frac{V_2}{V_1}\right)e^{j\Delta\phi} \quad (3a)$$

$$-Y_{D2}(\omega, V_2) = Y_{12}(\omega)\left(\frac{V_1}{V_2}\right)e^{-j\Delta\phi} + Y_{22}(\omega) \quad (3b)$$

where $\Delta\phi$ is the phase difference between the two voltage phasors of the array, i.e.,

$$\Delta\phi = \phi_2 - \phi_1. \quad (3c)$$

It is worth mentioning here that when only one element, say, element #1, is loaded with a negative conductance device, and the other is left unloaded or short circuited, (1) will result in

$$-Y_{D1}(\omega, V_1) = Y_{11}(\omega) - \frac{Y_{12}^2(\omega)}{Y_{22}(\omega)} \quad (4a)$$

or

$$-Y_{D1}(\omega, V_1) = Y_{11}(\omega). \quad (4b)$$

For the convenience of the following discussions, we define the above two cases as "open circuit free running" or "short circuit free running," respectively.

Theoretically, from (3a) and (3b), which are two complex equations and, thus, can yield four real equations, one can find all of the four circuit state variables, i.e., ω, V_1, V_2, and $\Delta\phi$ of the two-element array although all of the admittance functions, $Y_{D1}(\omega, V_1)$, $Y_{D2}(\omega, V_2)$, $Y_{11}(\omega)$, $Y_{12}(\omega)$, and $Y_{22}(\omega)$, in the above equations are usually too complicated to be given explicitly. However, in a symmetric two-element coupled negative conductance oscillator driven spatial power combining array, it is reasonable to assume that

$$V_1 = V_2 = V \quad (5a)$$

$$Y_{D1}(\omega, V_1) = Y_{D2}(\omega, V_2) = Y_D(\omega, V) \quad (5b)$$

$$Y_{11}(\omega) = Y_{22}(\omega). \quad (5c)$$

Therefore, (3a) and (3b) become

$$-Y_D(\omega, V) = Y_{11}(\omega) + Y_{12}(\omega)e^{j\Delta\phi} \quad (6a)$$

$$-Y_D(\omega, V) = Y_{12}(\omega)e^{-j\Delta\phi} + Y_{11}(\omega). \quad (6b)$$

The above two equations immediately lead to the following two ones

$$e^{j2\Delta\phi} = 1$$

or

$$e^{j\Delta\phi} = \pm 1 \quad (7a)$$

$$Y_D(\omega, V) + Y_{11}(\omega) \pm Y_{12}(\omega) = 0 \quad (7b)$$

which means that the symmetric two-element array has two operation modes, one in-phase, the other 180°-out-of-phase. The frequency and amplitude of each of the two modes of the array can be determined by solving (7b). This would require accurate modeling of the device and the antenna array.

Now, the question is how is the stability of the two modes of the symmetric two-element array. In order to answer this question, we differentiate the circuit equations (1a) and (1b) of the general two-element array to obtain

$$\left[\frac{\partial Y_1(\omega, V_1)}{\partial \omega}\Delta\omega_1 + \frac{\partial Y_1(\omega, V_1)}{\partial V_1}\Delta V_1\right]\tilde{V}_1 + \frac{\partial Y_{12}(\omega)}{\partial \omega} \cdot \Delta\omega_2\tilde{V}_2 + Y_1(\omega, V_1)\Delta\tilde{V}_1 + Y_{12}(\omega)\Delta\tilde{V}_2 = 0 \quad (8a)$$

$$\frac{\partial Y_{12}(\omega)}{\partial \omega}\Delta\omega_1\tilde{V}_1 + \left[\frac{\partial Y_2(\omega, V_2)}{\partial \omega}\Delta\omega_2 + \frac{\partial Y_2(\omega, V_2)}{\partial V_2}\Delta V_2\right] \cdot \tilde{V}_2 + Y_{12}(\omega)\Delta\tilde{V}_1 + Y_2(\omega, V_2)\Delta\tilde{V}_2 = 0 \quad (8b)$$

where

$$Y_1(\omega, V_1) = Y_{D1}(\omega, V_1) + Y_{11}(\omega) \quad (9a)$$

$$Y_2(\omega, V_2) = Y_{D2}(\omega, V_2) + Y_{22}(\omega) \quad (9b)$$

$$\begin{aligned}\Delta\tilde{V}_1 &= \Delta V_1 e^{j\phi_1} + V_1 e^{j\phi_1} j\,\Delta\phi_1\\ &= \tilde{V}_1(\Delta u_1 + j\,\Delta\phi_1)\end{aligned} \tag{9c}$$

$$\begin{aligned}\Delta\tilde{V}_2 &= \Delta V_2 e^{j\phi_2} + V_2 e^{j\phi_2} j\,\Delta\phi_2\\ &= \tilde{V}_2(\Delta u_2 + j\,\Delta\phi_2)\end{aligned} \tag{9d}$$

$$\Delta u_1 = \frac{\Delta V_1}{V_1} \tag{9e}$$

$$\Delta u_2 = \frac{\Delta V_2}{V_2} \tag{9f}$$

and, according to Kurokawa [18] and [19]

$$\Delta\omega_1 = \frac{\partial\Delta\phi_1}{\partial t} - j\,\frac{\partial\Delta u_1}{\partial t} \tag{9g}$$

$$\Delta\omega_2 = \frac{\partial\Delta\phi_2}{\partial t} - j\,\frac{\partial\Delta u_2}{\partial t}. \tag{9h}$$

Besides, from (1a), (1b), (9a), and (9b), we have

$$\frac{\tilde{V}_2}{\tilde{V}_1} = -\frac{Y_1(\omega, V_1)}{Y_{12}(\omega)} \tag{10a}$$

$$\frac{\tilde{V}_1}{\tilde{V}_2} = -\frac{Y_2(\omega, V_2)}{Y_{12}(\omega)}. \tag{10b}$$

From (8) and (10), we have

$$\frac{\partial Y_1(\omega, V_1)}{\partial\omega}\Delta\omega_1 + \frac{\partial Y_1(\omega, V_1)}{\partial V_1}\Delta V_1 + \frac{\partial Y_{12}(\omega)}{\partial\omega}\Delta\omega_2\left(\frac{\tilde{V}_2}{\tilde{V}_1}\right) + Y_1(\omega, V_1)\left[\left(\frac{\Delta\tilde{V}_1}{\tilde{V}_1}\right) - \left(\frac{\Delta\tilde{V}_2}{\tilde{V}_2}\right)\right] = 0 \tag{11a}$$

$$\frac{\partial Y_{12}(\omega)}{\partial\omega}\Delta\omega_1\left(\frac{\tilde{V}_1}{\tilde{V}_2}\right) + \frac{\partial Y_2(\omega, V_2)}{\partial\omega}\Delta\omega_2 + \frac{\partial Y_2(\omega, V_2)}{\partial V_2}\Delta V_2 + Y_2(\omega, V_2)\left[\left(\frac{\Delta\tilde{V}_2}{\tilde{V}_2}\right) - \left(\frac{\Delta\tilde{V}_1}{\tilde{V}_1}\right)\right] = 0 \tag{11b}$$

For the symmetric two-element array, we further have [from (7)]

$$\begin{aligned}\frac{\tilde{V}_2}{\tilde{V}_1} &= e^{j\,\Delta\phi}\\ &= \pm 1\\ &= e^{-j\,\Delta\phi}\\ &= \frac{\tilde{V}_1}{\tilde{V}_2}\end{aligned} \tag{12a}$$

$$\begin{aligned}Y_1(\omega, V_1) &= Y_2(\omega, V_2)\\ &= Y(\omega, V)\\ &= \mp Y_{12}(\omega).\end{aligned} \tag{12b}$$

Substituting (9c)–(9h) and (12) into (11), we obtain

$$\frac{\partial Y(\omega, V)}{\partial\omega}\left(\frac{\partial\Delta\phi_1}{\partial t} - j\,\frac{\partial\Delta u_1}{\partial t}\right) + V\,\frac{\partial Y(\omega, V)}{\partial V}\Delta u_1 \pm \frac{\partial Y_{12}(\omega)}{\partial\omega}\left(\frac{\partial\Delta\phi_2}{\partial t} - j\,\frac{\partial\Delta u_2}{\partial t}\right) \mp Y_{12}(\omega)(\Delta u_1 + j\,\Delta\phi_1 - \Delta u_2 - j\,\Delta\phi_2) = 0 \tag{13a}$$

$$\pm\frac{\partial Y_{12}(\omega)}{\partial\omega}\left(\frac{\partial\Delta\phi_1}{\partial t} - j\,\frac{\partial\Delta u_1}{\partial t}\right) + \frac{\partial Y(\omega, V)}{\partial\omega}\left(\frac{\partial\Delta\phi_2}{\partial t} - j\,\frac{\partial\Delta u_2}{\partial t}\right) + V\,\frac{\partial Y(\omega, V)}{\partial V}\Delta u_2 \mp Y_{12}(\omega)(\Delta u_2 + j\,\Delta\phi_2 - \Delta u_1 - j\,\Delta\phi_1) = 0 \tag{13b}$$

from which we further have

$$\frac{\partial}{\partial\omega}\begin{pmatrix} G & \pm G_{12} & B & \pm B_{12}\\ \pm G_{12} & G & \pm B_{12} & B\\ B & \pm B_{12} & -G & \mp G_{12}\\ \pm B_{12} & B & \mp G_{12} & -G\end{pmatrix}\cdot\frac{\partial}{\partial t}\begin{pmatrix}\Delta\phi_1\\ \Delta\phi_2\\ \Delta u_1\\ \Delta u_2\end{pmatrix} = \begin{pmatrix} \mp B_{12} & \pm B_{12} & \pm G_{12} - V\frac{\partial G}{\partial V} & \mp G_{12}\\ \pm B_{12} & \mp B_{12} & \mp G_{12} & \pm G_{12} - V\frac{\partial G}{\partial V}\\ \pm G_{12} & \mp G_{12} & \pm B_{12} - V\frac{\partial B}{\partial V} & \mp B_{12}\\ \mp G_{12} & \pm G_{12} & \mp B_{12} & \pm B_{12} - V\frac{\partial B}{\partial V}\end{pmatrix}\cdot\begin{pmatrix}\Delta\phi_1\\ \Delta\phi_2\\ \Delta u_1\\ \Delta u_2\end{pmatrix} \tag{14}$$

where the upper and lower signs of the elements in the matrices correspond to the in-phase and 180°-out-of-phase operation mode, respectively, besides

$$Y(\omega, V) = G(\omega, V) + jB(\omega, V) \tag{15a}$$

$$Y_{12}(\omega) = G_{12}(\omega) + jB_{12}(\omega) \tag{15b}$$

were used.

Finally, through matrix inversion and multiplication, (14) can be converted into the following form:

$$\begin{aligned}\frac{\partial}{\partial t}\begin{pmatrix}\Delta\phi_1\\ \Delta\phi_2\\ \Delta u_1\\ \Delta u_2\end{pmatrix} &= \kappa\cdot\left\{\begin{pmatrix}\alpha & -\alpha & \beta & -\beta\\ -\alpha & \alpha & -\beta & \beta\\ -\beta & \beta & \alpha & -\alpha\\ \beta & -\beta & -\alpha & \alpha\end{pmatrix} + \begin{pmatrix}0 & 0 & a & b\\ 0 & 0 & b & a\\ 0 & 0 & c & d\\ 0 & 0 & d & c\end{pmatrix}\right\}\cdot\begin{pmatrix}\Delta\phi_1\\ \Delta\phi_2\\ \Delta u_1\\ \Delta u_2\end{pmatrix}\\ &= \kappa\cdot\begin{pmatrix}\alpha & -\alpha & \beta + a & -\beta + b\\ -\alpha & \alpha & -\beta + b & \beta + a\\ -\beta & \beta & \alpha + c & -\alpha + d\\ \beta & -\beta & -\alpha + d & \alpha + c\end{pmatrix}\cdot\begin{pmatrix}\Delta\phi_1\\ \Delta\phi_2\\ \Delta u_1\\ \Delta u_2\end{pmatrix}\end{aligned} \tag{16a}$$

where

$$\kappa = \frac{1}{\left(\left|\frac{\partial Y}{\partial\omega}\right|^2 + \left|\frac{\partial Y_{12}}{\partial\omega}\right|^2\right)(1 - \rho^2)} \tag{16b}$$

$$\rho = \frac{2\left(\frac{\partial G}{\partial\omega}\frac{\partial G_{12}}{\partial\omega} + \frac{\partial B}{\partial\omega}\frac{\partial B_{12}}{\partial\omega}\right)}{\left|\frac{\partial Y}{\partial\omega}\right|^2 + \left|\frac{\partial Y_{12}}{\partial\omega}\right|^2} \tag{16c}$$

$$\alpha = \pm(1 \pm \rho)\left[G_{12}\frac{\partial(B \mp B_{12})}{\partial\omega} - B_{12}\frac{\partial(G \mp G_{12})}{\partial\omega}\right] \quad (16d)$$

$$\beta = \pm(1 \pm \rho)\left[G_{12}\frac{\partial(G \mp G_{12})}{\partial\omega} + B_{12}\frac{\partial(B \mp B_{12})}{\partial\omega}\right] \quad (16e)$$

$$a = -V\left[\frac{\partial G}{\partial V}\left(\frac{\partial G}{\partial\omega} - \rho\frac{\partial G_{12}}{\partial\omega}\right) + \frac{\partial B}{\partial V}\left(\frac{\partial B}{\partial\omega} - \rho\frac{\partial B_{12}}{\partial\omega}\right)\right] \quad (16f)$$

$$b = \pm V\left[\frac{\partial G}{\partial V}\left(\rho\frac{\partial G}{\partial\omega} - \frac{\partial G_{12}}{\partial\omega}\right) + \frac{\partial B}{\partial V}\left(\rho\frac{\partial B}{\partial\omega} - \frac{\partial B_{12}}{\partial\omega}\right)\right] \quad (16g)$$

$$c = -V\left[\frac{\partial G}{\partial V}\left(\frac{\partial B}{\partial\omega} - \rho\frac{\partial B_{12}}{\partial\omega}\right) - \frac{\partial B}{\partial V}\left(\frac{\partial G}{\partial\omega} - \rho\frac{\partial G_{12}}{\partial\omega}\right)\right] \quad (16h)$$

$$d = \pm V\left[\frac{\partial G}{\partial V}\left(\rho\frac{\partial B}{\partial\omega} - \frac{\partial B_{12}}{\partial\omega}\right) - \frac{\partial B}{\partial V}\left(\rho\frac{\partial G}{\partial\omega} - \frac{\partial G_{12}}{\partial\omega}\right)\right]. \quad (16i)$$

The stability of the two modes of the symmetric two-element array requires that the system of differential equations (16a) corresponding to the modes have stable solutions.

It is not difficult to show that

$$|\rho| \leq 1$$

thus

$$1 \pm \rho \geq 0$$

and

$$\kappa > 0.$$

Therefore, the system of differential equations (16a) yields stable solutions only when the matrix

$$[S] = \begin{pmatrix} \alpha & -\alpha & \beta + a & -\beta + b \\ -\alpha & \alpha & -\beta + b & \beta + a \\ -\beta & \beta & \alpha + c & -\alpha + d \\ \beta & -\beta & -\alpha + d & \alpha + c \end{pmatrix} \quad (17)$$

has nonpositive eigenvalues.

The eigenvalues of the matrix $[S]$ can be found to be

$$s_1 = 0 \quad (18a)$$

$$s_2 = c + d \quad (18b)$$

$$s_{3,4} = 2\alpha + \frac{c-d}{2} \pm \sqrt{\left(\frac{c-d}{2}\right)^2 - 2\beta(a-b) - 4\beta^2}. \quad (18c)$$

So, a mode of the symmetric two-element array is stable only when the following two conditions are satisfied, i.e.,

$$\text{I)} \quad c + d \leq 0 \quad (19a)$$

$$\text{II)} \quad 2\alpha + \frac{c-d}{2} < 0 \quad \text{when} \quad \delta < 0 \quad (19b)$$

or

$$2\alpha + \frac{c-d}{2} + \sqrt{\delta} \leq 0 \quad \text{when} \quad \delta \geq 0 \quad (19c)$$

where

$$\delta = \left(\frac{c-d}{2}\right)^2 - 2\beta(a-b) - 4\beta^2. \quad (19d)$$

From (16f)–(16i), we have

$$c + d = -V(1 \mp \rho)\left[\frac{\partial G}{\partial V}\frac{\partial(B \pm B_{12})}{\partial\omega} - \frac{\partial B}{\partial V}\frac{\partial(G \pm G_{12})}{\partial\omega}\right] \quad (20a)$$

$$c - d = -V(1 \pm \rho)\left[\frac{\partial G}{\partial V}\frac{\partial(B \mp B_{12})}{\partial\omega} - \frac{\partial B}{\partial V}\frac{\partial(G \mp G_{12})}{\partial\omega}\right] \quad (20b)$$

$$a - b = -V(1 \pm \rho)\left[\frac{\partial G}{\partial V}\frac{\partial(G \mp G_{12})}{\partial\omega} + \frac{\partial B}{\partial V}\frac{\partial(B \mp B_{12})}{\partial\omega}\right]. \quad (20c)$$

Therefore, the condition I (19a) is equivalent to

$$\frac{\partial G}{\partial V}\frac{\partial(B \pm B_{12})}{\partial\omega} - \frac{\partial B}{\partial V}\frac{\partial(G \pm G_{12})}{\partial\omega} > 0 \quad (21)$$

which is actually a more general form of the stability condition of a single oscillator, with a negative conductance device $Y_D(\omega, V)$ and an equivalent load $Y_{11}(\omega) \pm Y_{12}(\omega)$, given by Kurokawa [18].

Under the assumption that the admittance of the negative conductance device is a function of only the voltage magnitude, (21) becomes

$$\frac{\partial G_D}{\partial V}\frac{\partial(B_{11} \pm B_{12})}{\partial\omega} - \frac{\partial B_D}{\partial V}\frac{\partial(G_{11} \pm G_{12})}{\partial\omega} > 0. \quad (21a)$$

Graphically, the condition (21a) can be represented by

$$0^\circ < \theta < 180^\circ \quad (21b)$$

where θ is the angle from the device curve $-Y_D(\omega, V)$ to one of the load curves $Y_{11}(\omega) \pm Y_{12}(\omega)$ at their corresponding solution points as shown in Fig. 2(a). Also shown in Fig. 2(a) are the load curves and their corresponding solution points of an open circuit free running element and a short circuit free running element. For "weak coupling" case as will be discussed immediately below, the above conditions (21) can be expected to be satisfied for all of the four solutions simultaneously. That is to say, one stable solution will most likely mean that the other three solutions will also be stable (although their corresponding frequency and amplitude will be slightly different from one another). However, for "nonweak coupling" cases, this is not necessarily true.

As for the condition II), the situation is generally more involved. Now, if we consider only the "weak coupling" case, i.e., the coupling, or mutual admittance $Y_{12}(\omega)$, between the two elements in the symmetric two-element array is very small, or, it satisfies

$$|Y_{12}(\omega)| \ll |Y_{11}(\omega)| \quad (22a)$$

$$\left|\frac{\partial G_{12}}{\partial\omega}\right| \ll \left|\frac{\partial G}{\partial\omega}\right| \quad (22b)$$

$$\left|\frac{\partial B_{12}}{\partial\omega}\right| \ll \left|\frac{\partial B}{\partial\omega}\right| \quad (22c)$$

$$|2\beta(a-b) + 4\beta^2| \approx |2\beta(a-b)| \ll \left(\frac{c-d}{2}\right)^2. \quad (22d)$$

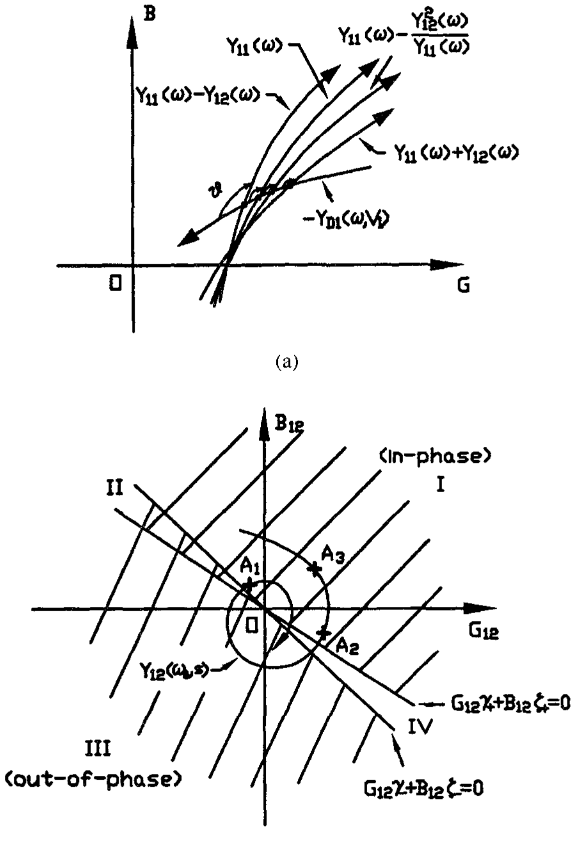

(a)

(b)

Fig. 2. Graphical representation of the modes and their stability of a symmetric two-element weakly coupled negative conductance oscillator driven spatial power combining array: (a) condition I) and (b) condition II).

Then, we will have

$$c - d = -V(1 \pm \rho)\left[\frac{\partial G}{\partial V}\frac{\partial (B \mp B_{12})}{\partial \omega} - \frac{\partial B}{\partial V}\frac{\partial (G \mp G_{12})}{\partial \omega}\right]$$
$$\approx \frac{1 \pm \rho}{1 \mp \rho}(c + d) < 0 \tag{23a}$$

and the condition II) can be simplified into the following form:

$$2\alpha + \frac{c-d}{2} + \left|\frac{c-d}{2}\right| \cdot \left[1 - \frac{4\beta(a-b)}{(c-d)^2}\right] < 0$$

or

$$\alpha + h_{\pm}\beta < 0 \tag{23b}$$

where

$$h_{\pm} = \frac{a-b}{c-d} = \frac{\dfrac{\partial G}{\partial V}\dfrac{\partial (G \mp G_{12})}{\partial \omega} + \dfrac{\partial B}{\partial V}\dfrac{\partial (B \mp B_{12})}{\partial \omega}}{\dfrac{\partial G}{\partial V}\dfrac{\partial (B \mp B_{12})}{\partial \omega} - \dfrac{\partial B}{\partial V}\dfrac{\partial (G \mp G_{12})}{\partial \omega}} \approx \frac{\dfrac{\partial G}{\partial V}\dfrac{\partial G}{\partial \omega} + \dfrac{\partial B}{\partial V}\dfrac{\partial B}{\partial \omega}}{\dfrac{\partial G}{\partial V}\dfrac{\partial B}{\partial \omega} - \dfrac{\partial B}{\partial V}\dfrac{\partial G}{\partial \omega}}. \tag{23c}$$

Substituting (16d) and (16e) into (23b), we obtain

$$\pm(G_{12}\gamma_{\pm} + B_{12}\zeta_{\pm}) < 0 \tag{24}$$

or

$$G_{12}\gamma_{+} + B_{12}\zeta_{+} < 0 \quad \text{for in-phase mode} \tag{24a}$$
$$G_{12}\gamma_{-} + B_{12}\zeta_{-} > 0 \quad \text{for 180°-out-of-phase mode} \tag{24b}$$

where

$$\gamma_{\pm} = h_{\pm}\frac{\partial G}{\partial \omega} + \frac{\partial B}{\partial \omega} \tag{24c}$$
$$\zeta_{\pm} = -\frac{\partial G}{\partial \omega} + h_{\pm}\frac{\partial B}{\partial \omega}. \tag{24d}$$

Because $h_{+} \neq h_{-}$ (thus, $\gamma_{+} \neq \gamma_{-}$ and $\zeta_{+} \neq \zeta_{-}$), the above conditions divide the whole G_{12}–B_{12} plane into four regions as schematically shown in Fig. 2(b). In region I)

$$G_{12}\gamma_{+} + B_{12}\zeta_{+} < 0$$
$$G_{12}\gamma_{-} + B_{12}\zeta_{-} < 0$$

thus, only the in-phase mode is stable. In region II)

$$G_{12}\gamma_{+} + B_{12}\zeta_{+} < 0$$
$$G_{12}\gamma_{-} + B_{12}\zeta_{-} > 0$$

thus, both the in-phase and 180°-out-of-phase modes are stable. In region III)

$$G_{12}\gamma_{+} + B_{12}\zeta_{+} > 0$$
$$G_{12}\gamma_{-} + B_{12}\zeta_{-} > 0$$

thus, only the 180°-out-of-phase mode is stable. In region IV)

$$G_{12}\gamma_{+} + B_{12}\zeta_{+} > 0$$
$$G_{12}\gamma_{-} + B_{12}\zeta_{-} < 0$$

thus, neither of the two modes is stable.

On the other hand, because $h_{+} \approx h_{-}$ (thus, $\gamma_{+} \approx \gamma_{-}$ and $\zeta_{+} \approx \zeta_{-}$), the regions II) and IV) are expected to be much smaller than the regions I) and III). Therefore, in most symmetric two-element weakly coupled negative conductance oscillator driven spatial power combining arrays, either the in-phase mode [region I)] or the 180°-out-of-phase mode [region III)] will easily be obtained while the mode jumping and unstable oscillations will hardly be observed.

As an example also shown in Fig. 2(b) is a typical locus of the mutual admittance $Y_{12}(\omega_0, s)$ of a symmetric two-element free space radiation coupled negative conductance oscillator driven spatial power combining array. A definite description of the relationship between $Y_{12}(\omega_0, s)$ and s (the separation between the two element antennas) would depend on the actual structure of the specific active antenna array. However, due to the free space radiation nature of the mutual coupling between the two antenna elements in the specific active antenna array, one may qualitatively have

$$Y_{12}(\omega_0, s) \propto \frac{1}{s}e^{-jk_0 s}$$
$$k_0 = \omega_0\sqrt{\varepsilon_0\mu_0}.$$

Therefore, a clockwise inward spiral curve in Fig. 2(b) is appropriate to schematically describe the behavior of the

$Y_{12}(\omega_0, s)$. This schematic picture can lead to the following conclusions for this specific active antenna array.

1) When the separation between the two antenna elements changes by one free space wavelength, the locus will travel a complete circle through all the four regions. This will result in periodic mode (phase) alternating and, at some points, unstable oscillations. Besides, the frequency and amplitude of the specific active antenna array will also experience alternating changes with the separation due to their dependence on $Y_{12}(\omega_0, s)$ (7b), thus, the separation, s.
2) The spatial alternating period of the mode (phase), frequency and amplitude of the specific active antenna array would be about one free space wavelength.
3) A stable in-phase mode can always be found within a separation range of about half a free space wavelength.
4) When the operating mutual admittance $Y_{12}(\omega_0, s)$, such as point A_1 or A_2 in the figure, is very close to the boundaries defined by those $\gamma_\pm$ and $\zeta_\pm$, which are functions of the bias voltages of the negative conductance devices for a given array circuit, changing the bias voltages may also change the positions of the boundaries and, at worst, lead to mode jumping. This kind of mode jumping is not desired especially in bias tuning frequency modulated transmitter applications. Technically, this possibility can be avoided by any means which changes the relative positions of the operating mutual admittance point and the boundaries in the G_{12}–B_{12} plane such that the operating mutual admittance, e.g., the point A_3 in the figure, is located far away from the boundaries. In the specific case under discussion where the operating mutual admittance can be easily changed with the separation between the two antenna elements, this objective can be attained by choosing an appropriate separation. Experimentally, one can change the separation between the two active antenna elements while monitoring the oscillation of the array [8]. From the experiment, the most favorable separation for the stable operation of the specific free space radiation coupled oscillator driven spatial power combining array can be determined.

Our experiments done at C band with symmetric two-element weakly coupled Gunn oscillator driven spatial power combining arrays with different separations between the two elements also demonstrated the validity of the above theoretical analysis to a certain extent.

III. Experimental Results

In our experiments, an E-plane oriented symmetric two-element coupled Gunn oscillator driven spatial power combining array as shown in Fig. 3 was used. Each of the two element circuits in the array utilized a circular microstrip ring as the resonant unit of the oscillator, and a slot on the ground plane of the substrate coupled with the circular microstrip ring as the radiating antenna. The mutual coupling (admittance) is fulfilled through mainly the climbing waves on the radiating ground plane and the surface waves in the substrate. Two Gunn diodes were mounted between the ring and the ground plane of the substrate at the outer sides of the two rings of the array and shared the same bias voltage in order to ensure symmetry and good heat sinking. A metal mirror block is introduced one quarter wavelength behind the rings to avoid any back scattering. The design of the element circuit has been experimentally optimized for MA49135 Gunn diodes and RT/Duroid 5880 substrate (thickness = 1.57 mm, ε_r = 2.20) [20].

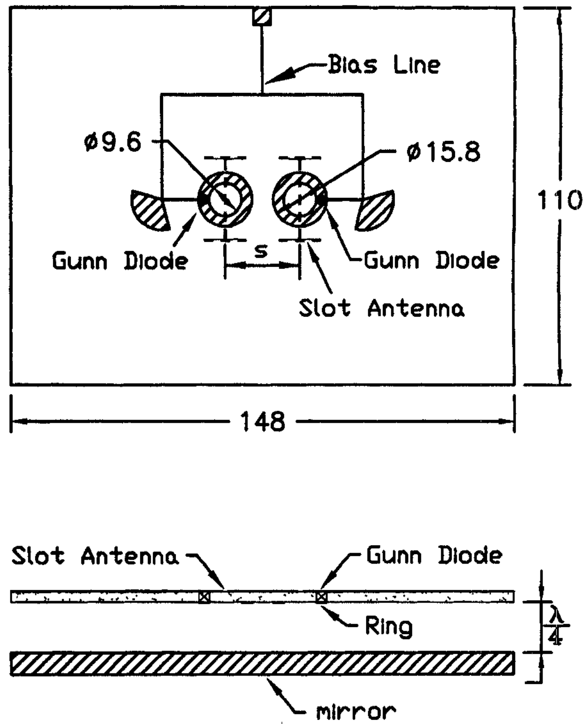

Fig. 3. Experimental circuit design (all dimensions are in millimeters).

Under weak coupling conditions, according to the previous analysis, the oscillating frequency of the array depends mainly on the element circuit, and the phase relationship of the array on the mutual admittance between the two elements. From antenna and propagation theory and the nature of the mutual coupling, the mutual admittance between the two element circuits in the experimental structure will change with the separation as discussed at the end of Section II. Therefore, in order to show the two different stable phase relationships of the active antenna array, different separations were used. On the other hand, from phased array theory, grating lobes will emerge for separation larger than half free space wavelength between the two elements. Taking some power, the grating lobes will reduce the power combining efficiency of the active antenna array along the main beam direction, thus, in view of spatial power combining, are not desired. Therefore, a practical symmetric two-element coupled Gunn oscillator driven spatial power combining array should be able to operate at the in-phase mode with separation less than half free space wavelength between the two elements.

The frequency of the experimentally optimized C-band element circuit was around 6.0 GHz, thus, the half free space wavelength is 25 mm. The maximum dimension of the element circuit along the E-plane direction, which determines the minimum separation between the two element circuits in the E-plane oriented array, is the outer diameter, 15.8 mm, of the microstrip ring resonator. Between 15.8 mm and 25 mm, four representative separations, 16, 19, 22, and 25 mm were used in the design of the passive portions of four symmetric two-element coupled Gunn oscillator driven spatial power combining arrays.

The passive portions of the four active antenna arrays of different separations were fabricated at the center on four rectangular RT/Duroid 5880 substrate sheets of area $110\,\text{mm}\,(2.2\lambda_0) \times 150\,\text{mm}\,(3.0\lambda_0)$. With two Gunn diodes mounted on one of the four passive arrays as described previously, a two-element coupled Gunn oscillator driven spatial power combining array can be formed. In order to ensure the symmetry of the active antenna arrays, which is part of the assumption in the previous analysis, Gunn diodes were specifically ordered from M/A-COM in a batch and the passive portions of the active antenna arrays were fabricated by means of photoetching technique. Despite these efforts, the symmetry of the active antenna arrays remains a problem due to the inconsistency of the Gunn diodes and the passive element circuits.

It is not difficult to understand that, for an ideal symmetric two-element coupled Gunn oscillator driven spatial power combining array with a common bias line as used in our circuit design, each of the two elements shall have the same open circuit free running output power and frequency as the other at a certain bias voltage. Therefore, the bias tuning characteristics of the open circuit free running output power and frequency of the two elements in the same array were used to measure the symmetry of the two-element coupled Gunn oscillator driven spatial power combining array. Here, the open circuit free running condition instead of the short circuit free running condition is used because the later will also short the DC bias and is thus not desired in our experiments.

With the help of the measured bias tuning characteristics of the open circuit free running output power and frequency of different Gunn diode and passive element circuit combinations, appropriate combinations were found which would result in approximately symmetric two-element coupled Gunn oscillator driven spatial power combining arrays. Experiments done with these approximately symmetric two-element coupled Gunn oscillator driven spatial power combining arrays showed that:

1) $s = 16$ mm circuits easily yielded the stable 180°-out-of-phase operation when loaded with two "well-matched" (i.e., they, with their respectively loaded passive element circuits, well satisfied the symmetry condition) Gunn diodes;
2) $s = 19$, 22, and 25 mm circuits easily yielded the stable in-phase operation when loaded with two "well-matched" Gunn diodes.

The phase relationship of the above approximately symmetric two-element arrays were determined from their measured E-plane patterns. Along the normal direction of the slot-radiating ground plane, a "zero" or a maximum radiation indicates the 180°-out-of-phase or in-phase operation, respectively. The measured E-plane patterns of the approximately symmetric two-element arrays for $s = 25$ and 16 mm are shown in Figs. 4 and 5. For comparison, the E-plane pattern of a typical open circuit free running element is also shown in these figures.

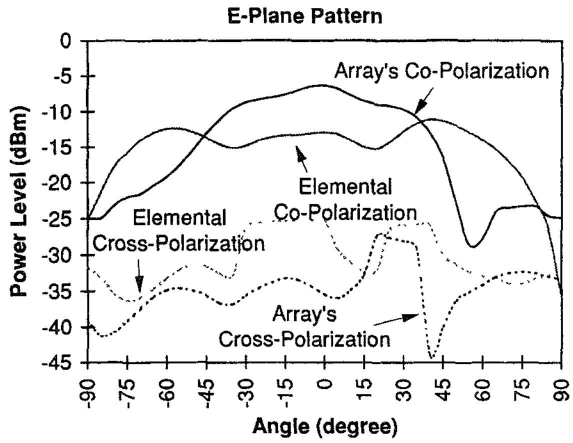

Fig. 4. E-plane pattern of the symmetric two-element coupled negative conductance oscillator driven spatial power combining array working at in-phase mode ($s = 25$ mm).

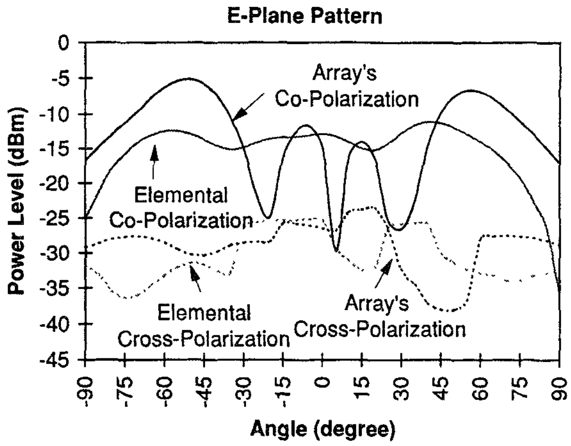

Fig. 5. E-Plane pattern of the symmetric two-element coupled negative conductance oscillator driven spatial power combining array working at 180°-out-of-phase mode ($s = 16$ mm).

All of the above measurements were made in a mini anechoic chamber system developed in our laboratory. As shown in Fig. 6, the system consists of a mobile mini anechoic chamber with inner space about $0.6\,\text{m} \times 0.6\,\text{m} \times 1.6\,\text{m}$, a WYSE 386/80 personal computer, an HP6642A DC power supply, an ORIEL step motor, an HP8562A spectrum analyzer, two HP437B power meters, and three Narda 642A standard gain horns. At one end of the chamber, a horizontally turnable axle connected with the step motor protrudes in the chamber from top to the center position. The active antenna under test is mounted on the axle in the chamber. At the other end of the chamber, about 1.50 m apart from the active antenna, two horns connected with the two power meters are oriented such that one horn receives only the vertically polarized radiation and the other horn receives only the horizontally polarized

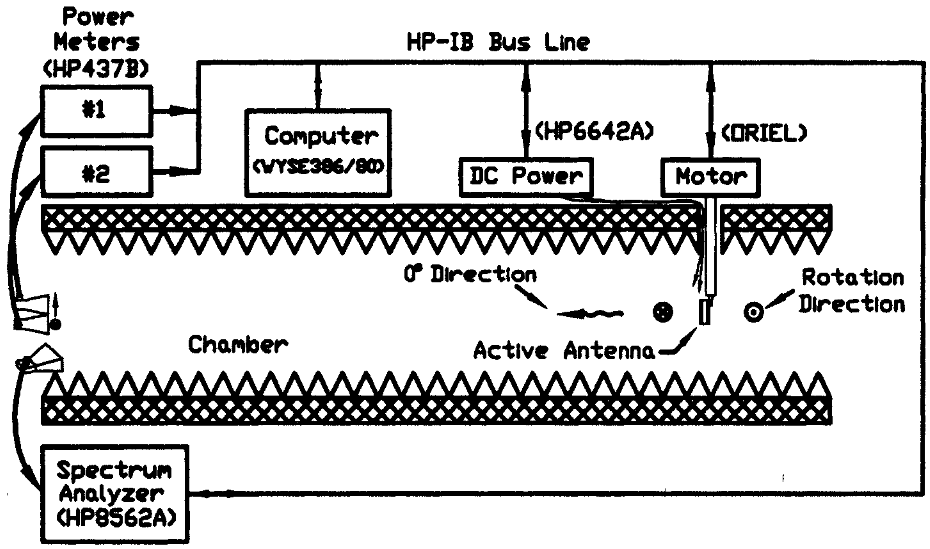

Fig. 6. Mini anechoic chamber system setup.

radiation. Located at an appropriate position near the two horns in the chamber, the third horn is connected to and picks up certain radiation power for the spectrum analyzer. The frequency and stability of the active antenna is monitored through the display of the spectrum analyzer. The computer controls the output voltage of the DC power supply applied to the active antenna and the revolution of the step motor and takes the power data from the power meters. Finally, the measured vertical and horizontal polarization pattern data of the active antenna are stored in a user defined data file for further processing.

Because the separation between the two elements in our experimental circuits could not be varied continuously, only four representative separations were used in our experiments. From the experimental results, one can infer the following.

1) The $s = 16$ mm array worked in region III) (180° out-of-phase) and the $s = 19$, 22, and 25 mm arrays in region I) (in-phase).
2) A mode jumping occurred somewhere between $s = 16$ and 19 mm.

The mode overlapping region II) and the unstable oscillation region IV) were not demonstrated in our experiments because the regions II) and IV) are very small. However, the mode jumping and unstable oscillation regions were all experimentally observed by continuously varying the separation between the two antenna elements [8] or the bias voltage of the active devices [10] in different symmetric two-element weakly coupled oscillator driven spatial power combining arrays.

IV. Conclusion

From the preceding analysis and experiments, we can conclude the following.

1) A symmetric two-element coupled negative conductance oscillator driven spatial power combining array has two stable modes, one in-phase, the other 180°-out-of-phase.
2) The mutual admittance between the two elements in the symmetric two-element coupled negative conductance oscillator driven spatial power combining array plays an important role in deciding if the array is stable or not and which stable mode the array will take.

The above analytical conclusions are well verified by the previously reported experimental and simulation work [8], [10], [16], and the experimental work documented in this paper. It is also worth noting that

1) Two terms, "free running (elements)" and "weak coupling," which were frequently seen without clear quantitative definitions in previous literature on coupled negative conductance oscillator driven spatial power combining arrays, were explicitly defined in the preceding discussions.
2) The theory developed in this paper holds for all symmetric two-element coupled negative conductance oscillator driven spatial power combining arrays no matter whether two terminal active devices, such as Gunn diodes, or three terminal active devices, such as FET, are used in the arrays. It also covers mutual coupling of any (weak, intermediate, or strong) magnitudes although only the weak coupling case was considered in more detail in the preceding discussions.
3) Theory on the modes and their stability of any (symmetric or asymmetric) coupled negative conductance oscillator driven spatial power combining array with more than two elements can be developed from similar procedure as outlined in this paper. A complete theory like the one presented in this paper is very important in the development of the coupled negative conductance oscillator driven spatial power combining array technology.

Acknowledgment

The experimental assistance of L. Fan is greatly appreciated.

REFERENCES

[1] K. Chang and C. Sun, "Millimeter-wave power-combining techniques," *IEEE Trans. Microwave Theory Tech.,* vol. MTT-31, no. 2, pp. 91–107, Feb. 1983.

[2] J. W. Mink, "Quasi-optical power combining of solid-state millimeter-wave sources,"*IEEE Trans. Microwave Theory Tech.*, vol. MTT-34, no. 2, pp. 273–279, Feb. 1986.

[3] D. Staiman, M. E. Breese, and W. T. Patton, "New technique for combining solid-state sources," *IEEE J. Solid-State Circuits,* vol. SC-3, no. 3, pp. 238–243, Sept. 1968.

[4] M. F. Durkin, R. J. Eckstein, M. D. Mills, and M. S. Stringfellow, "35 GHz active aperture," in *IEEE MTT-S Int. Microwave Symp. Dig.,* June 1981, pp. 425–427.

[5] R. J. Dinger, D. J. White, and D. Bowling, "A 10 GHz space power combiner with parasitic injection locking," in *IEEE MTT-S Int. Microwave Symp. Dig.,* June 1986, pp. 163–166.

[6] K. D. Stephan, "Inter-injection-locked oscillators for power combining and phased arrays," *IEEE Trans. Microwave Theory Tech.,* vol. MTT-34, no. 10, pp. 1017–1025, Oct. 1986.

[7] S.-L. Young, and K. D. Stephan, "Radiation coupling of inter-injection-locked oscillators," *SPIE Millimeter Wave Technology IV and Radio Frequency Power Sources (1987),* vol. 791, pp. 69–76.

[8] K. D. Stephan and S.-L. Young, "Mode stability of radiation-coupled interinjection-locked oscillators for integrated phased arrays," *IEEE Trans. Microwave Theory Tech.,* vol. 36, no. 5, pp. 921–924, May 1988.

[9] K. A. Hummer and K. Chang, "Spatial power combining using active microstrip patch antennas," *Microwave Opt. Tech. Lett.,* vol. 1, no. 1, pp. 8–9, Mar. 1988.

[10] K. Chang, K. A. Hummer, and J. L. Klein, "Experiments on injection locking of active antenna elements for active phased arrays and spatial power combiners," *IEEE Trans. Microwave Theory Tech.,* vol. 37, no. 7, pp. 1078–1084, July 1989.

[11] R. A. York and R. C. Compton, "Quasi-optical power combining using mutually synchronized oscillator arrays," *IEEE Trans. Microwave Theory Tech.,* vol. 39, no. 6, pp. 1000–1009, June 1991.

[12] ——, "Measurement and modeling of radiative coupling in oscillator arrays," *IEEE Trans. Microwave Theory Tech.,* vol. 41, no. 3, pp. 438–444, Mar. 1993.

[13] R. A. York, "Nonlinear analysis of phase relationships in quasi-optical oscillator arrays," *IEEE Trans. Microwave Theory Tech.,* vol. 41, no. 10, pp. 1799–1809, Oct. 1993.

[14] S. Nogi, J. Lin, and T. Itoh, "Mode analysis and stabilization of a spatial power combining array with strongly coupled oscillators," *IEEE Trans. Microwave Theory Tech.,* vol. 41, no. 10, pp. 1827–1837, Oct. 1993.

[15] J. Lin and T. Itoh, "Two-dimensional quasi-optical power-combining arrays using strongly coupled oscillators," *IEEE Trans. Microwave Theory Tech.,* vol. 42, no. 4, pp. 734–741, Apr. 1994.

[16] B. Toland, J. Lin, B. Houshmand, and T. Itoh, "Electromagnetic simulation of mode control of a two element active antenna," in *1994 IEEE MTT-s Dig.,* 1994, pp. 883–886.

[17] X.-D. Wu and K. Chang, "Novel active FET circular patch antenna arrays for quasi-optical power combining," *IEEE Trans. Microwave Theory Tech.,* vol. 42, no. 5, pp. 766–771, May 1994.

[18] K. Kurokawa, "Some basic characteristics of broadband negative resistance oscillator circuits," *Bell Syst. Tech. J.,* vol. 48, pp. 1937–1955, July/Aug. 1969.

[19] ——, "The single-cavity multiple-device oscillator," *IEEE Trans. Microwave Theory Tech.,* vol. MTT-19, no. 10, pp. 793–801, Oct. 1971.

[20] Z. Ding, L. Fan, and K. Chang, "A new type of active antenna for coupled gunn oscillator driven spatial power combining arrays," *IEEE Microwave and Guided Wave Lett.,* vol. 5, no. 8, pp. 246–248, Aug. 1995.

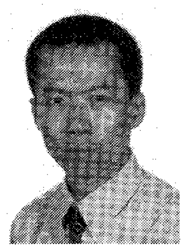

Zhengping Ding (S'94) received the B.Eng.E.E. degree from Tsinghua University, Beijing, China, the M.S. degree from Beijing Institute of Technology, Beijing, China in 1984 and 1987, respectively.

From 1987 to 1992, he was with Xian Research Institute of Electromechanical Information Technology, Xian, China, where he was involved in the research and development of microwave telemetry and millimeter wave radar systems. Since 1993, he has been pursuing the Ph.D. degree at Texas A&M University, College Station, TX, where he has been involved in the research and development of microwave active antennas and spatial power combining technology as well as electromagnetic field analysis of a microstrip-line-to-waveguide coupling structure.

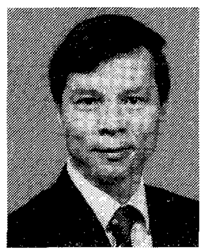

Kai Chang (S'75–M'76–SM'85–F'91) received the B.S.E.E. degree from the National Taiwan University, Taipei, Taiwan, the M.S. degree from the State University of New York at Stony Brook, and the Ph.D. degree from the University of Michigan, Ann Arbor, in 1970, 1972, and 1976, respectively.

From 1972 to 1976, he worked for the Microwave Solid-State Circuits Group, Cooley Electronics Laboratory of the University of Michigan as a Research Assistant. From 1976 to 1978, he was employed by Shared Applications, Inc., Ann Arbor, where he worked in computer simulation of microwave circuits and microwave tubes. From 1978 to 1981, he worked for the Electron Dynamics Division, Hughes Aircraft Company, Torrance, CA, where he was involved in the research and development of millimeter-wave solid-state devices and circuits, power combiners, oscillators and transmitters. From 1981 to 1985, he worked for the TRW Electronics and Defense, Redondo Beach, CA, as a Section Head, developing state-of-the-art millimeter-wave integrated circuits and subsystems including mixers, VCO's, transmitters, amplifiers, modulators, upconverters, switches, multipliers, receivers, and transceivers. He joined the Electrical Engineering Department of Texas A&M University in August 1985 as an Associate Professor and was promoted to a Professor in 1988. In January 1990, he was appointed E-Systems Endowed Professor of Electrical Engineering. His current interests are in microwave and millimeter-wave devices and circuits, microwave integrated circuits, integrated antennas, wideband and active antennas, phased arrays, microwave power transmission, and microwave optical interactions. He authored and coauthored several books *Microwave Solid-State Circuits and Applications* (New York: Wiley, 1994), *Microwave Ring Circuits and Antennas* (New York: Wiley, 1996), and *Integrated Active Antennas and Spatial Power Combining* (New York: Wiley, 1996). He served as the editor of the four-volume *Handbook of Microwave and Optical Components* (New York: Wiley, 1989 and 1990). He is the editor of the IEEE TRANSACTIONS ON MICROWAVE AND OPTICAL TECHNOLOGY LETTERS and the Wiley Book Series in Microwave and Optical Engineering. He has published more than 250 technical papers and several book chapters in the areas of microwave and millimeter-wave devices, circuits, and antennas.

Dr. Chang received the Special Achievement Award from TRW in 1984, the Halliburton Professor Award in 1988, the Distinguished Teaching Award in 1989, the Distinguished Research Award in 1992, and the TEES Fellow Award in 1996 from the Texas A&M University. He is a Fellow of IEEE.